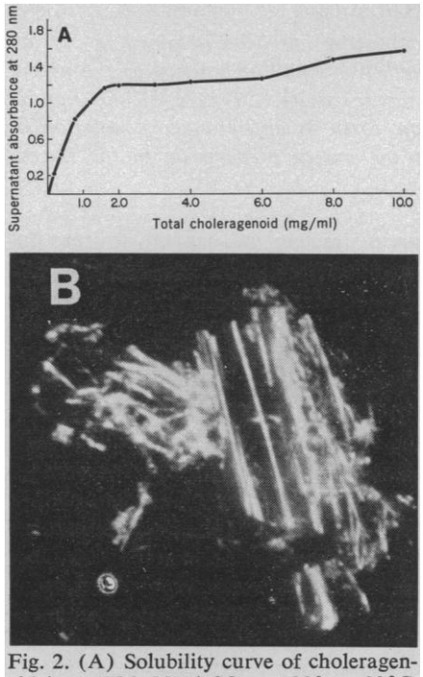

Fig. 2. (A) Solubility curve of choleragenoid in 2.67*M* $(NH_4)_2SO_4$, at 22° to 23°C. (B) Crystals of choleragenoid, same conditions as Fig. 1B.

for the most part, the crystals tended to assume the plate or rhomboidal form predominant in Fig. 1B. After the initial crystallization, it was possible to obtain more crystals by seeding fresh $(NH_4)_2SO_4$-treated preparations. Crystals were harvested by centrifugation, redissolved, and dialyzed against tris buffer. The potency of the redissolved choleragen was tested, in parallel with the parent toxin, for choleragenicity in infant rabbits (*6*), for skin reactivity in adult rabbits (*7*), and by the Lf test (*8*). The results in each case were identical with the parent toxin. The dose causing a mean choleragenic score (*1, 6*) of 5 was estimated from titrations in groups of five infant rabbits each, to be 0.4 μg. The skin reactive dose was between 0.0003 and 0.001 μg, determined in duplicate titrations in each of two rabbits. [This dose was somewhat higher than that which we reported previously (*2*), but we have found that results of this test vary depending on the sensitivity of the rabbits used on a given occasion.] The Lf dose, as already reported (*8*), was 1.0 μg. Disc electrophoresis revealed a single protein band in the separating gel with a trace of aggregated material which failed to penetrate the polyacrylamide gel.

Choleragenoid was processed similarly, except that a higher concentration of $(NH_4)_2SO_4$, 2.67*M*, was used in the solubility test. The results (Fig. 2A) indicated that choleragenoid was not homogeneous according to this criterion. A gradual curve was observed with increasing absorbance at high concentrations of protein. This is entirely consistent with our previous observations that there are multiple species of choleragenoid (*2*). Nevertheless, using $(NH_4)_2SO_4$ at the isoelectric point, *p*H 7.75, of the predominant species of choleragenoid (*2*), we were able to obtain crystals (Fig. 2B) which resembled those of choleragen. In this case, however, a slight amount of amorphous precipitate was removed after the first $(NH_4)_2SO_4$ addition, and crystallization was achieved after a subsequent increase of the $(NH_4)_2SO_4$ concentration to approximately 2.7*M*. Disc electrophoresis of the redissolved crystalline material suggested that it consisted primarily of the predominant choleragenoid species (*2*). The Lf dose of the redissolved crystals was identical with the parent preparation of choleragenoid, 0.6 μg (*8*). We believe this to be the first time that crystallization of a natural toxoid has been reported.

In addition to showing that the cholera toxin, like diphtheria, tetanus, and other classical bacterial toxins, is crystallizable, our results indicate that we were working with a pure protein. Our study reemphasizes the differences between our previous work and that of investigators working with cruder preparations (*3*) who reported dissociation of diarrheagenic activity and skin reactivity. We can conclude only that the discrepancies are attributable to the use of impure preparations or to the possibility that in the procedures used, which resulted in losses of most of the original toxic activity (*3*), fractions or subunits of the toxin molecule may have been separated perhaps in combination with other materials present. Although we have demonstrated the heterogeneity of the subunits of the choleragen molecule (*9, 10*), we have thus far been unable to separate the subunits and thereby evaluate this hypothesis. In contrast to previous reports on less pure materials (*11*), chemical analyses (*10*) indicate that the purified products are simple proteins essentially free of lipid and carbohydrate.

RICHARD A. FINKELSTEIN
JOSEPH J. LOSPALLUTO
Departments of Microbiology and *Biochemistry, University of Texas Southwestern Medical School, Dallas 75235*

References and Notes

1. R. A. Finkelstein and J. J. LoSpalluto, *J. Exp. Med.* **130**, 185 (1969).
2. ———, *J. Infec. Dis.* **121** (Suppl.), S63 (1970).
3. A. C. Lewis and B. A. Freeman, *Science* **165**, 808 (1969); G. F. Grady and M. C. Chang, *J. Infec. Dis.* **121** (Suppl.), S92 (1970).
4. R. A. Finkelstein, J. W. Peterson, J. J. LoSpalluto, *J. Immunol.* **106**, 868 (1971).
5. R. A. Finkelstein, K. Fujita, J. J. LoSpalluto, *ibid.* **107**, 1043 (1971).
6. R. A. Finkelstein, J. J. Jehl, A. Goth, *Proc. Soc. Exp. Biol. Med.* **132**, 835 (1969).
7. J. P. Craig, in *Microbial Toxins*, S. Kadis, T. C. Montie, S. J. Ajl, Eds. (Academic Press, New York, 1971), vol. 2A, p. 189.
8. R. A. Finkelstein, *Infec. Immun.* **2**, 691 (1970).
9. J. J. LoSpalluto and R. A. Finkelstein, *Fed. Proc.* **30**, 304a (1971).
10. ———, *Biochim, Biophys. Acta*, in press.
11. W. H. Coleman, J. Kaur, M. E. Iwert, G. J. Kasai, W. Burrows, *J. Bacteriol.* **96**, 1137 (1968); J. Kaur, H. C. König, W. R. Martin, W. Burrows, *J. Infec. Dis.* **121**, 78 (1970); S. H. Richardson and D. J. Evans, Jr., *J. Bacteriol.* **96**, 1443 (1968).
12. We thank Dr. Iwao Kato who set an example in his purification and crystallization of diphtheria toxin; see I. Kato, H. Nakamura, T. Uchida, J. Koyama, T. Katsura, *Japan. J. Exp. Med.* **30**, 129 (1960).
13. We thank Barbara Smith, Judith Head, and Katherine Grundman for technical assistance. Supported by PHS research grant AI-08877 under the United States–Japan Cooperative Medical Science Program administered by the National Institute of Allergy and Infectious Diseases.

9 July 1971

Microsomal Lipid Peroxidation: Morphological Characterization

Abstract. *Lipid peroxidation of liver and kidney microsomes induces a highly characteristic sequence of morphological changes typified by detachment of ribosomes and formation of large aggregates of vesicles bound together by dense amorphous material and myelin figure-like debris. The trilaminar structure of the membrane is, however, retained even after complete peroxidation, though its spacing may be increased. The aggregates resemble lysosomal lipofuscin pigment as well as the membranous aggregates of endoplasmic reticulum seen in the liver after carbon tetrachloride poisoning.*

Lipid peroxidation of cell membranes may play an important, although for the present poorly understood, role in many types of cell injury. It has been detected, by chemical means, in the liver after administration of toxic compounds; in the brain, muscle, and liver of vitamin E–deficient rats, and in the kidneys of choline-deficient rats (*1*). It may also be associated with radiation

injury, in aging processes, in hyperbaric effects, and in acute ethanol intoxication (*1*, *2*).

In vitro, lipid peroxidation occurs when liver mitochondria or microsomes are incubated in the presence of various redox agents such as ferrous ions, mercurial compounds, hemoproteins, ascorbate, and cystamine (*3*). Despite growing knowledge of the chemistry of lipid peroxidation lesions, the morphological alterations which occur in peroxidation have not been characterized. Characterization of these alterations would not only aid understanding of the pathogenesis of peroxidation lesions but would also provide new means for detecting lipid peroxidation in intact tissues, in which the lipid peroxidation end products may be rapidly metabolized. Hence we have studied the morphological alterations which occur in microsomes during in vitro peroxidation. We chose the hepatic microsomal fraction for this study, since the endoplasmic reticulum is especially vulnerable to peroxidation because it contains an electron-transfer system that can catalyze lipid-peroxidation reactions (*2–4*).

Liver or kidney was removed quickly from young male rats, immersed in 0.25*M* ice-cold sucrose, weighed, and homogenized. The nuclei, mitochondria, and lysosomes were removed, and the microsomes were then sedimented at 105,000*g* for 60 minutes in a Beckman model L2-50 ultracentrifuge with a No. 30 fixed-angle rotor. The microsomes (2 mg of microsomal protein per milliliter) were incubated at 37°C, in a Clarke-type oxygen electrode, in 3 ml of the following medium: 0.025*M* tris-HCl buffer (final *p*H 7.4), 0.15*M* KCl, 5 μM glucose-6-phosphate, 10 μl of glucose-6-phosphate dehydrogenase (Sigma type 10), and 16.7 m*M* nicotinamide. After a steady tracing was obtained, 10 μl of reduced nicotinamide adenine dinucleotide (NADPH), 15 m*M* (for a final concentration of 50 μM) was added; then 5 μl of a solution containing 0.6*M* adenosine diphosphate (ADP) and 6 m*M* $FeCl_3$ (for a final concentration of 1 m*M* ADP and 0.01 m*M* Fe) was added in order to start lipid peroxidation (*1*, *4*, *5*). Lipid peroxidation was followed for 50 minutes by continuously measuring the rate of oxygen consumption and the amount of peroxidation end product, malonaldehyde, before addition of ADP-Fe and at 5-minute intervals after peroxidation started. The addition of NADPH alone, without the NADPH regenerating system, to the medium did not increase

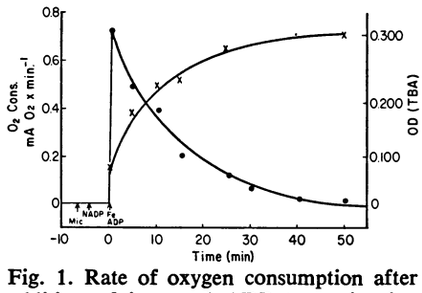

Fig. 1. Rate of oxygen consumption after addition of iron and ADP to an incubation medium containing liver microsomes. The formation of malonyldialdehyde was measured by the thiobarbituric acid (*TBA*) test and is plotted on the scale at the right.

oxygen consumption, which continued at approximately the same rate for 20 minutes and slowly leveled off after 50 minutes (Fig. 1). The malonyldialdehyde formation, as measured by the thiobarbituric acid test, steadily increased during peroxidation and after complete peroxidation was about sixfold higher than the control values (Fig. 1).

In order to study the morphological changes during in vitro peroxidation, control and peroxidized microsomes were fixed for electron microscopy by adding an aliquot of the incubation mixture to an equal amount of fixative. The fixative was a 1 : 1 mixture of 4 percent glutaraldehyde and 4 percent formaldehyde buffered with 0.1*M* Na-cacodylate to *p*H 7.4. The microsomes were fixed for 2 hours (24°C), collected on Millipore filters (pore size 0.22 μm), and washed overnight in 0.25*M* cacodylate buffer containing 8 percent sucrose, and post-osmicated in 1 percent *s*-collidine buffered O_sO_4 (*p*H 7.4) for 1 hour. The filters were then dehydrated in a series of ethanols and flat-embedded in Epon. Fragments of embedded sheets were reembedded in slots in Epon blocks and sectioned in the plane normal to the surface of the filters. The sections were double stained with uranyl acetate and lead citrate.

In electron micrographs the control microsomes appeared as a population of small vesicles about 0.5 μm in diameter, many of which were studded with ribo-

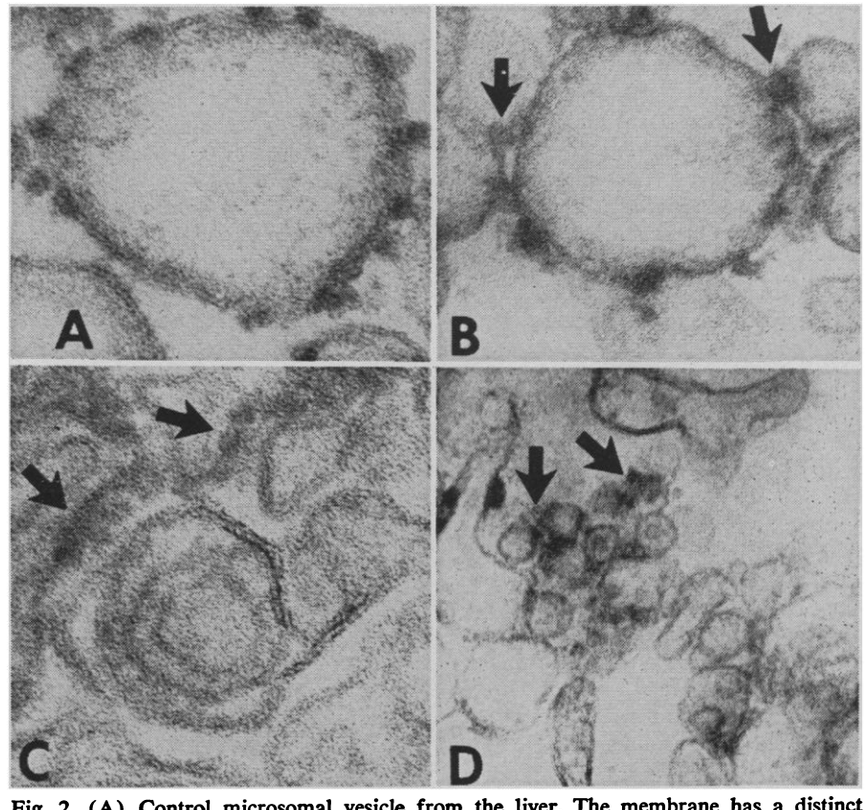

Fig. 2. (A) Control microsomal vesicle from the liver. The membrane has a distinct trilaminar appearance, and there are numerous ribosomes on the surface (× 225,000). (B) Microsomal vesicle after 15 minutes of peroxidation. The ribosomes have usually disappeared and larger, homogeneous densities (arrows) seem to attach adjacent vesicles to one another (× 155,000). (C) Liver microsomal membrane at higher magnification after 50 minutes of peroxidation. The membranes are irregular, and there is flocculent material between them (arrows). However, the trilaminar structure is still apparent (× 210,000). (D) Kidney microsomes after peroxidation for 25 minutes. The vesicles are irregular and are bound together with dense, amorphous material (arrows) (× 63,000).

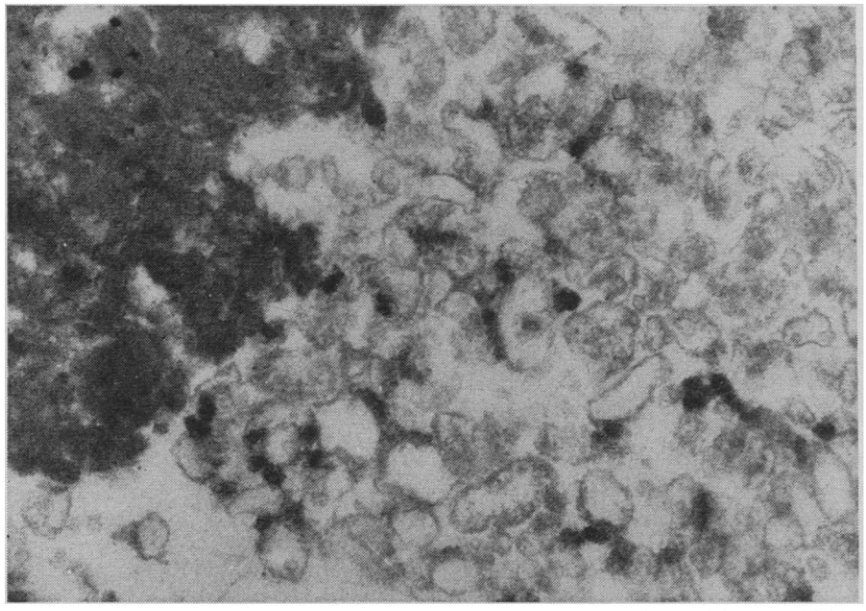

Fig. 3. Liver microsomes after peroxidation for 50 minutes. The vesicles are highly irregular and abundant, dense amorphous material is present around them and in a large aggregate at upper left (× 95,000).

somes (Fig. 2A). The majority of them were round or slightly oval. The membranes displayed a distinct trilaminar structure with a mean peak-to-peak thickness of about 50 Å. Flocculent material and occasional small vesicles were seen within the microsomal vesicles. Contaminating mitochondria, lysosomes, and microbodies were infrequent. After peroxidation for 10 to 15 minutes, the microsomal vesicles were less regular in shape and contained less flocculent material. Although ribosomes were still on the surface of many vesicles, there were others in which dense amorphous material was seen on the outer surface of the vesicles in place of ribosomes (Fig. 2B). After peroxidation for 20 minutes, the microsomes often appeared as aggregates of tightly packed tubules or vesicles, among which amorphous dense material and membranous debris were present. At higher magnification the vesicles were irregular in shape and tightly packed together. Often the individual vesicles were attached to one another by amorphous dense material. Ribosomes were only infrequently found, either free between the vesicles or on their surface. After 50 minutes these changes were even more pronounced and the amount of amorphous material was increased (Figs. 2C and 3). With kidney microsomes the oxygen consumption proceeded at a high rate for about 25 minutes and then leveled off. At that time the malonyldialdehyde values were increased about twofold as compared with the control values. When we studied the peroxidized microsomes by electron microscopy, sequences of alterations essentially similar to those in liver microsomes were observed (Fig. 2D). These can be summarized as follows: (i) detachment of ribosomes from the surface of the vesicles, followed by decomposition and complete disappearance of ribosomes; (ii) gradual change in the shape of microsomes from regular round vesicles to less regular profiles; and (iii) appearance of dense amorphous precipitate and membranous debris with myelin-like figures in the space between the vesicles.

At low magnification these aggregates also resembled the lysosomal aging pigment or lipofuscin found in a variety of tissues such as heart and brain (Fig. 3). The similarity of peroxidation end products to lipofuscin has been recently verified on the basis that lipid peroxidation of subcellular organelles gives fluorescent products with fluorescence and excitation spectra similar to those of lipofuscin pigments (*6*).

In electron micrographs taken at a higher magnification, it was obvious that both liver and kidney microsomes had retained their trilaminar membrane structure even after complete peroxidation, although the membrane thickness sometimes seemed to be increased. (Fig. 2, C and D). This result agrees with our previous findings that trilaminar membrane structure is preserved even after removal of over 90 percent of phospholipids (*5*), and with previous observations of Napolitano *et al.* (*7*). Therefore, it further supports the hypothesis that membrane-associated lipids are not essential for the trilaminar pattern of membranes as seen in electron microscopy (*8*). Control preparations, incubated without NADPH, maintained essentially normal ultrastructure and showed none of these changes. Lipid peroxidation in vitro thus induces distinct alterations in the structure of liver and kidney microsomes, best characterized by the formation of densely packed aggregates of vesicular and tubular structures bound together with amorphous material. This is of considerable interest since we and others have found morphologically identical lesions in liver poisoned with carbon tetrachloride (*9*), where in vivo lipid peroxidation has been clearly demonstrated (*1*). The relation of these to lipid peroxidation was, however, not suggested previously. Whether the formation of tubular aggregates is specific for lipid peroxidation is unknown. However, this assumption is supported by the finding that morphologically similar lesions have also been described after phosphorus and iodoform poisoning in the liver (*10*), conditions which have been suggested as being associated with lipid peroxidation. In addition, Gritzka and Trump (*11*) have found similar tubular aggregates in the kidney after mercuric chloride poisoning. If the presence of tubular aggregates is highly characteristic of lipid peroxidation, then one should also detect lipid peroxidation in the kidneys after poisoning with mercuric chloride. Although this question has not been decided, Utley *et al.* (*12*) have shown that in vitro incubation of microsomes with mercuric chloride results in formation of lipid peroxides.

A. U. Arstila
Mary A. Smith
B. F. Trump

Department of Pathology, University of Maryland School of Medicine, Baltimore 21201

Notes and References

1. A. K. Ghoshal and R. O. Recknagel, *Life Sci.* **4**, 2195 (1965); R. O. Recknagel, *Pharmacol. Rev.* **19**, 145 (1967); A. A. Barber and F. Bernheim, *Advan. Gerontol. Res.* **2**, 355 (1967); A. J. Monserrat, A. K. Ghoshal, W. S. Hartroft, E. A. Porta, *Amer. J. Pathol.* **55**, 163 (1969); D. A. Sell and E. S. Reynolds, *J. Cell Biol.* **41**, 736 (1969).
2. P. Hochstein, in *Third International Conference on Hyperbaric Medicine* (National Academy of Sciences, Washington, D.C., 1969), p. 64; L. Packer, D. W. Deamer, R. L. Health, *Advan. Gerontol. Res.* **2**, 77 (1967).
3. A. K. Schneider, E. E. Smith, F. E. Hunter,

Jr., *Biochemistry* **3**, 1470 (1964); P. Hochstein, K. Nordenbrand, L. Ernster, *Biochem. Biophys. Res. Commun.* **14**, 323 (1964); W. D. Cash, M. Gardy, H. E. Carlson, E. A. Ekong, *J. Biol. Chem.* **241**, 1745 (1966); B. O. Christopherson, *Biochem J.* **106**, 515 (1968); E. D. Wills, *ibid.* **113**, 325, 333 (1969).
4. S. Orrenius, G. Dallner, L. Ernster, *Biochem. Biophys. Res. Commun.* **14**, 329 (1964); Z. A. Placer, L. L. Cushman, B. C. Johnson. *Anal. Biochem.* **16**, 359 (1966).
5. B. F. Trump, S. M. Duttera, W. L. Byrne, A. U. Arstila, *Proc. Nat. Acad. Sci. U.S.* **66**, 433 (1970).
6. K. S. Chio, U. Reiss, B. Fletcher, A. L. Tappel, *Science* **166**, 1535 (1969).
7. L. Napolitano, F. Lebaron, J. Scaletti, *J. Cell Biol.* **34**, 817 (1967).
8. E. D. Korn, *Fed. Proc.* **28**, 6 (1969); S. B. Fleischer, F. Fleischer, W. Stoeckenius, *J. Cell Biol.* **32**, 193 (1967); W. Stoeckenius and E. M. Engleman, *ibid.* **42**, 613 (1969).
9. E. A. Smuckler and M. Arcasoy, *Int. Rev. Exp. Pathol.* **7**, 305 (1969); B. F. Trump and A. U. Arstila, in *Principles of Pathobiology*, M. F. La Via and R. B. Hill Jr., Eds. (Oxford Univ. Press, New York, 1971), pp. 9–95; A. U. Arstila and M. A. Smith, *Fed. Proc.* **30**, 569 (1971).
10. M. Bassi, *Exp. Cell Res.* **20**, 313 (1960); E. S. Reynolds, *J. Cell Biol.* **19**, 139 (1963).
11. T. D. Gritzka and B. F. Trump. *Amer. J. Pathol.* **52**, 1225 (1968).
12. H. S. Utley, F. Bernheim, P. Hochstein, *Arch. Biochem. Biophys.* **118**, 29 (1967).
13. Supported by grant AM 10698 to B. F. Trump and grants from Sigrid Juselius Foundation and Finnish National Research Council for Medical Sciences to A.U.A.

30 July 1971

Opossum Fetuses Grown in Culture

Abstract. *Opossum fetuses explanted at limb bud stages have been successfully grown in culture for periods up to 20 hours. Blood circulation was maintained, and organogenesis continued at about the same rate as in vivo.*

Despite the obvious advantages for observation and experiment of growing mammalian fetuses in culture, few successful methods have yet been devised. The main difficulty appears to be failure to provide any adequate substitute in culture for the allantoic placenta or to support the growth of this placenta if it is explanted with the fetus. Some workers have maintained the isolated fetus in conditions adequate for certain physiological studies (*1, 2*) but such "cultures" have not usually resulted in growth or differentiation.

Only in rodents has there been much success in obtaining fetal development. The explanted rat fetus, for example, can now be grown for periods up to 2 or 3 days at any time between the primitive streak (8th gestation day) and 55-somite, limb bud (14th day) stages of development (*3*). Rodents are unusual among eutherian mammals in that during the early stages of organogenesis the respiratory and nutritional needs of the fetus are mediated entirely by a yolk-sac placenta; only later does the allantoic placenta become functional. The yolk-sac placenta is a relatively simple structure, and when explanted with the early fetus it grows and develops a blood circulation in a manner very similar to that in vivo. Hence the rodent fetus can grow and differentiate in culture until such time as the allantoic placenta becomes indispensable.

In view of these findings it seemed desirable to examine the behavior in culture of embryos from a mammal that does not have a complex allantoic placenta and that relies almost entirely on a yolk sac. Such a mammal is the opossum *Didelphys marsupialis virginiana* (Kerr), a marsupial common in North America. The embryonic development of the opossum has been described in detail by McCrady (*4*). The gestation period is 12¾ days, and the young are born at a stage of development corresponding about to that of the mouse fetus of the same age (or rat fetus of 14 days) except that the forelimbs, lungs, pancreas, and a few other organs are precociously developed (Fig. 1). The allantois is present only as a simple sac that enlarges with urine during the last 3 days of gestation and probably has no placental function. But the yolk sac, which in rats is about 7 mm in diameter on the 13th day of gestation, develops in the opossum to over 20 mm in diameter, with folds closely adhering to those of the uterine endometrial surface.

Although the opossum breeds erratically in captivity and is much more difficult to maintain in self-perpetuating colonies than the common laboratory animals, a reliable method has been developed for obtaining embryos of predetermined age from recently captured opossums (*5*). The animals are trapped during the breeding season, at which time practically all the females either have young in the pouch or within a few days give birth to litters sired in the wild. If the young are removed from the pouch, a postlactational estrus follows a week later. This estrus is of exceptional intensity, and when the females are caged with males a high proportion of fertile matings can usually be achieved; the females that fail to mate at this estrus may do so at the end of the next cycle 28 days later. Because the young can be removed from the pouch at any desired time the method is very convenient for initiating timed pregnancies as required.

In the present study 12 females, newly trapped in Florida, were purchased from a dealer during February

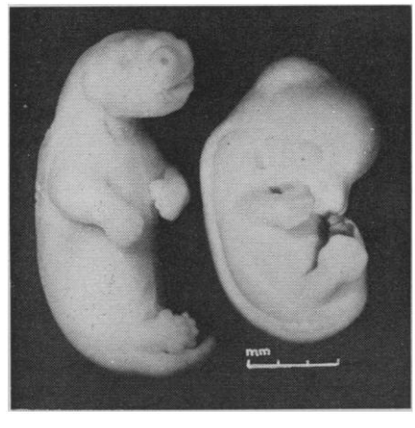

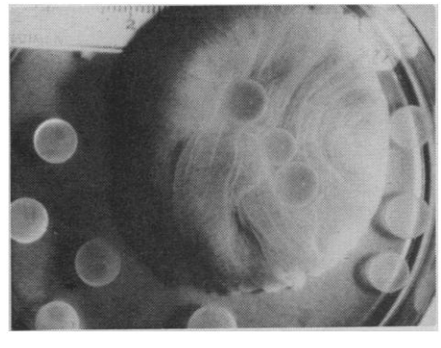

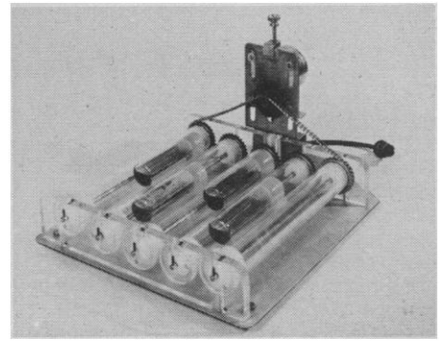

Fig. 1 (top left). Newborn opossum (left) and 14-day rat fetus (right) at same magnification. Forelimbs and parts of the head of the opossum are very advanced, but hindlimbs are only slightly more developed than in rat; tail is shorter. Fig. 2 (top right). Opened opossum uterus at 8 to 9 days of pregnancy. At this stage the embryos lie free in the uterine cavity. Fig. 3 (bottom right). Apparatus for rotating culture tubes.